Hyposensitive canopy conductance renders ecosystems vulnerable to extreme droughts

Hang Xu
Beijing Forestry University https://orcid.org/0000-0002-6661-3139
Zhiqiang Zhang (zhqzhang@bjfu.edu.cn)
College of Water and Soil Conservation, Beijing Forestry University, Beijing 100083, China
https://orcid.org/0000-0002-0083-7455
Ram Oren
Duke University https://orcid.org/0000-0002-5654-1733
Xiaoyun Wu
Beijing Forestry University

Article

Keywords: atmospheric evaporative demand, canopy stomatal conductance, drought, ecosystem vulnerability, FLUXNET, water-use strategy

Posted Date: October 6th, 2021

DOI: https://doi.org/10.21203/rs.3.rs-912317/v1

Abstract

Increased drought intensity with rising atmospheric demand for water (hereafter VPD) increases the risk of tree mortality worldwide. Ecosystem-scale water-use strategy (WUS_e), quantified here by canopy stomatal sensitivity to VPD (S_c), is increasingly recognized as a factor in drought-related ecosystem dysfunction. However, the links between S_c and ecosystem adaptation to and stability following droughts are poorly established. We examined how S_c regulates carbon sequestration, identifying ecosystems potentially susceptible to drought-induced mortality based on data from the global flux network, remote-sensing products, and plant functional-traits archive. We found that S_c is higher where ecosystem water availability is low in arid regions, reflecting conservative WUS_e (i.e., hypersensitivity), but ecosystems of all regions converge on permissive WUS_e (i.e., hyposensitivity) under ample water supply. During extreme droughts, hyposensitive and hypersensitive ecosystems achieved similar net ecosystem productivity employing considerably different structural-functional strategies. However, hyposensitive ecosystems, risking their hydraulic system with permissive WUS_e, did not recover from extreme droughts as quickly. Models predicting current performance and future distributions of vegetation types should account for the greater vulnerability of hyposensitive ecosystems to intensifying atmospheric and soil drought.

Full Text

Worldwide increases in plant mortality events have been associated with extreme stress conditions caused by intensifying climate variations[1–3]. In turn, severe mortality events affect regional carbon, water, and energy cycling by altering biosphere-atmosphere exchange processes, potentially perturbing regional to global climate systems, exacerbating the severity, frequency, and extent of climatic extremes[4,5]. Indeed, no specific vegetation type or climate zone is safe from the effects of predicted future warming and droughts, even in regions historically endowed with ample water[6,7], yet some may be better equipped to withstand such pressures. However, current specifications of dynamic global vegetation models do not account for the wide variance among plant hydraulic properties and their water use strategies, rendering plant mortality predictions uncertain[8,9]. Therefore, understanding the coupled response of carbon sequestration and water consumption to climate-induced stress and identifying species and ecosystems particularly vulnerable to climate extremes are essential for accurate predictions of future vegetation dynamics and distributions[10,11].

Drought has been, and will remain one of the major threats to humans and the natural systems[12,13]. Observational and modeling studies have demonstrated that increasing atmospheric aridity, indicated by vapor pressure deficit (VPD), is chief among drought-related constraints to terrestrial carbon sinks and ecosystem function[14,15]. When climate regimes are localized, less affected by air masses from drier or wetter regions, high VPD and low soil moisture are correlated over the range of soil moisture below which stomatal conductance is affected[16]. In the context of climate change, ecosystem-scale stomatal response to decreasing soil moisture and increasing VPD is much more pronounced than observed

responses to increasing atmospheric [CO_2][17]. Indeed, progressive change in climate, during which the feedback between soil water and VPD drives increasingly drying terrestrial surfaces and more severe plant water stress, could cause abrupt and irreversible shifts in biotic communities, affecting their biodiversity, ecosystem functions, and carbon storage[4,18]. Correspondingly, the way plants respond to the variation of atmospheric demand for moisture, especially under droughts, determines community resilience and stability.

Plant water-use strategies largely determine the tradeoff between carbon uptake and water use[19,20]. At the ecosystem scale, there is no definitive evidence that water-use strategy (WUS_e) is a vital mechanism of drought response strategy. However, the role of WUS_e in the maintenance of ecosystem functions during extreme droughts and the recovery following droughts has not been well assessed[24]. Furthermore, hydraulic behavior is largely considered fixed to a species[21,22]. However, evidence is mounting that plant hydraulic behavior is the product of the interaction of biology and growth environment[20]. We propose that the sensitivity of canopy stomatal conductance (G_c) to VPD (S_c) is a factor contributing to the sustainability and resilience of ecosystems encountering droughts[14]. Along a continuum of S_c, ecosystems may experience varying degrees of carbon starvation or hydraulic failure under water-limited conditions[23]. Here, we used S_c to explore how WUS_e regulates carbon sequestration during droughts and predict the potential drought-induced risk of ecosystem dysfunction worldwide.

Canopy stomatal sensitivity regulated by water availability in arid regions

We evaluated WUS_e based on canopy stomatal response to VPD relative to a theoretical response, one consistent with the role of stomata in regulating the xylem water potential (Ψ_x), thus protecting its hydraulic function[25]. The *normalized deviation* from theoretical canopy stomatal sensitivity to VPD[25], S_c (see Fig. 4 in Methods) was used to classify ecosystems as hypersensitive when positive (>1.05 the theoretical) and hyposensitive when negative (<0.95 the theoretical), the latter consistent with anisohydric behavior. We consider S_c in the intermediate range as consistent with isohydric behavior, consistent with conservative regulation of Ψ_x. The average empirical ratio of $dG_c/dln(VPD)$ (m) to reference canopy stomatal conductance (G_{cref}, i.e., conductance at VPD = 1 kPa) was 0.62 ± 0.01 $ln(kPa)^{-1}$ (mean ± standard error) across all 165 sites, smaller than expected (0.64 ± 0.01; $p < 0.001$, paired t-*test*), yet larger than the ratio determined by porometric and sap flow methods, and based on hydraulic theory[25] (0.60; $p = 0.003$, one-sample t-*test*). The distribution of S_c was fairly uniform for each ecosystem type, ranging mostly between −0.2 to 0.2 (Fig. 1a). For wetlands and croplands, the empirical m/G_{cref} was significantly lower than the theoretical ratio ($p = 0.001$ and 0.003, respectively), and S_c was lower than that of other ecosystems ($p < 0.05$). Although this may suggest highly anisohydric behavior (i.e., weak regulation of Ψ_x), reflected in hyposensitivity of stomatal conductance to VPD, it is more likely that evaporation of free water from open water, and wet soil and canopy (even though precipitation effects were removed),

introduced a VPD-dependent bias in estimates of canopy-scale stomatal conductance based on eddy covariance data. Thus, we excluded these ecosystems from further analyses. Among the remaining datasets, there was no difference in S_c between angiosperm- and gymnosperm-dominated ecosystems (p = 0.102; Fig. 1b).

At several flux sites, the normalized slope of G_c to VPD changed with soil moisture[14]; we found that S_c decreased with multi-year mean ecosystem water availability (α) only in arid regions (Fig. 1c). Although the range of data from humid regions was shifted to slightly greater water availability, ecosystems in both arid and humid regions may experience α ranging from ample to limiting. S_c exponentially varied with α in arid regions (p < 0.001), increasing from −0.044 at α = 0.8, to 0.061 at α = 0.3 (Fig. 1c). In contrast, S_c was insensitive to the range of α in humid regions (p = 0.925), remaining stable at around −0.025. Thus, ecosystems in arid and humid regions shared S_c at high α, but clearly separated as water availability decreased.

The prevailing water conditions control not only ecosystem functions but also plant xylem structure and hydraulic conductivity[26], jointly determining WUS_e. In relatively arid sites, S_c varied with α within a narrow range of soil moisture[27]. Thus, for a given site, WUS_e depends on plant hydraulic characteristics and long-term environmental conditions[19,20], changing relatively little even in drought years, as indicated by m and G_{cref} decreasing proportionally during droughts (Supplementary Fig. 1). Although we found no evidence that WUS_e was affected by ecosystem type (Fig. 1a) or ecosystem-scale hydraulic traits (as reflected in plant xylem type; Fig. 1b), WUS_e was considerably influenced by the prevailing habitat water availability in arid regions only (Fig. 1c). For ecosystems in humid regions, permissive WUS_e prevails regardless of available moisture, perhaps reflecting acclimation to lesser atmospheric demand for moisture. It is notable that in arid regions, where habitat moisture was not very limiting (α > 0.5), hyposensitive ecosystems showing permissive WUS_e were ~2.2-fold more common than hypersensitive ecosystems of conservative WUS_e, while the ecosystems with the conservative behavior were ~1.7-fold more common in drier habitats.

Ecosystem water-use strategies under droughts

Water-deficit stress lowered G_{cref} (z-score) in moderate and extreme droughts (Fig. 2a), independent of the climatic region, suggesting that some loss of hydraulic conductivity in the soil-plant pathway occurs under drought. Although G_{cref} anomaly was linearly related to the intensity of droughts regardless of WUS_e, hyposensitive ecosystems showed greater sensitivity than hypersensitive ecosystems (p = 0.038, ANCOVA; Fig. 2a). Thus, although there was no difference in the G_{cref} anomaly between the two types of ecosystems during moderate droughts (p = 0.695), hyposensitive ecosystems showed more negative G_{cref} anomaly than hypersensitive ecosystems during extreme droughts (p = 0.047). Consistent with the canopy stomatal conductance response to drought, the annual net ecosystem productivity (NEP) of most ecosystems decreased with drought intensity (Fig. 2b). Focusing on hypersensitive and hyposensitive

ecosystems, the slope of the linear relationship between NEP anomaly (z-score) and drought severity was 1.17 and 1.11, respectively, showing similar sensitivity (p = 0.899, ANCOVA). Too few data preclude a firm conclusion, but extreme droughts seem to impact NEP of hyposensitive ecosystems less than hypersensitive ecosystems during the drought year. Drought intensity noticeably affected the ratio of leaf area index (LAI) to NEP (Fig. 2c). The LAI/NEP anomaly of the two types of ecosystems was similar at low drought intensity and very different under extreme drought conditions. Specifically, under extreme drought conditions, the mean LAI/NEP anomaly for hyposensitive ecosystems was 0.64 ± 0.15 and remained high as drought intensified, but declined in hypersensitive ecosystems to an average of −0.08 ± 0.07.

Combined with the responses of G_{cref}, LAI/NEP, and NEP to drought intensity, hypersensitive and hyposensitive ecosystems achieve similar net carbon uptake through very different responses: Hypersensitive ecosystems respond to droughts through a reduction of LAI, allowing the residual foliage to maintain higher conductance, thus reducing the impact on NEP, while hyposensitive ecosystems show a permissive WUS_e, hanging onto their inefficient leaves, potentially with a lesser impact on NEP. Thus, both ecosystem types meet increasing drought severity with decreasing rate of carbohydrate production, yet in very different states: Hypersensitive with lower LAI potentially at its maximum efficiency; hyposensitive maintaining high LAI of very low efficiency.

Moreover, G_{cref} of most hypersensitive ecosystems (91%) recovered to its multi-year non-drought mean the following year, but that of the majority (67%) of hyposensitive ecosystems, including all those experiencing extreme droughts, did not (Supplementary Fig. 2). Indeed, the ratio of G_{cref} following droughts to that of non-drought years across all hypersensitive ecosystems (1.02 ± 0.03), similar to that of isohydric systems (1.00 ± 0.07), was not different from unity (p = 0.357), while that of the hyposensitive ecosystems (0.90 ± 0.02) was lower (p = 0.001; Fig. 3a), indicating that hyposensitive ecosystems likely experienced a substantial loss of hydraulic conductance (e.g., cavitation, embolism, root surface-area decline) during droughts. Although LAI/NEP of the year following a drought year recovered to a normal state, NEP of hyposensitive ecosystems was still less than the multi-year non-drought level (0.84 ± 0.07; p = 0.040; Fig. 3a). Consequently, few hypersensitive ecosystems show carryover effects of droughts, while the cost of permissive WUS_e was a failure of most hyposensitive ecosystems to recover fully from droughts.

Consistent with these findings, moving from ecosystems with conservative WUS_e to those less regulated, as indicated by lower S_c (see Fig. 1c), ecosystem resistance (R_t) and recovery (R_c) displayed divergent trends (Fig. 3b). Specifically, R_c increased (R^2 = 0.27, p < 0.001) while R_t sharply decreased (R^2 = 0.23, p = 0.002) with S_c across all ecosystems. When S_c is between 0.04 and 0.16, the difference between R_t and R_c is the smallest, delineating the range in which the ability of an ecosystem to both persist and recover from droughts to its long-term quasi-stable equilibrium is balanced (Fig. 3b). We note that this region is occupied by hypersensitive ecosystems, while hyposensitive ecosystems display higher R_t but lower R_c. Therefore, the results suggest that hyposensitive ecosystems, behaving consistently with anisohydric

hydraulics, recover slower from a drought year due to the increased hydraulic resistance of the soil-plant pathway.

Hyposensitive ecosystems at risk of mortality under extreme droughts

Although drought can cause substantial stress to plants, with potential physiological, biochemical, and morphological effects[11], their impact on ecosystem functions ranges from none to severe depending on drought intensity and duration as well as WUS_e. We found that moderate-intensity drought did not greatly impact ecosystem carbon sequestration and hydraulic functions, and the responses were similar in hyposensitive and hypersensitive ecosystems (Fig. 2). However, when ecosystems experienced extreme drought stress, hyposensitive and hypersensitive ecosystems exhibited different structural and functional strategies despite a relatively similar decline in carbon sequestration (Fig. 2). Specifically, hypersensitive ecosystems decreased the degree of carbon starvation caused by extreme droughts, reducing the proportion of structural carbohydrates aboveground (e.g., LAI) while increasing leaf carbon sequestration efficiency (Fig. 2c). Reducing LAI by shoot and leaf dieback are strategies that improve the water supply to the residual foliage[28], maintaining conductance and photosynthetic rates while permitting higher partitioning of photosynthates to non-structural carbohydrates (NSC, e.g., sugars and starch) in support of plant metabolism and osmolality[29]. Such loss of canopy elements may reflect a conservative behavior when biochemical regulations are insufficient to withstand extreme droughts. This behavior, reflected in yellowing foliage following a few weeks of severe drought, is commonly observed in ecosystems composed of fast-growing species of high gas-exchange leaves[30], representing a preference for cutting losses short, giving up return on carbon invested in a portion of foliage rather than risk the entire hydraulic system and mortality if droughts persist. In contrast, hyposensitive ecosystems kept their LAI as drought severity increased, thus keeping photosynthetically less efficient foliage, a strategy that may allow recouping the investment in foliage over the short term, but risking the hydraulic system and future carbon uptake.

The question remaining is, which strategy may be more detrimental to plant survival and ecosystem stability not only during droughts, but in subsequent years. We found no difference between hyposensitive and hypersensitive ecosystems in ecosystem-scale P_{50} (i.e., Ψ_x at which 50% loss of conductivity) and hydraulic safety margin (HSM) (Supplementary Fig. 3). Although NEP of the ecosystems with different WUS_e responded to droughts in a similar way, the consequences of their strategies reflect diverging effects on ecosystem stability and resilience, at least during the year following droughts. A mechanism advanced in support of less strict stomatal regulation is the prevention of drought-induced carbon starvation, but this may result in hydraulic failure and a cascade of consequences[23]. A number of studies documented drought-induced tree mortality often associated with substantial loss of hydraulic conductivity, yet plant death was not uniformly caused by insufficient NSC because carbohydrate distribution and allometric growth changed with drought[2,31]. Indeed, these two attributes may be feeding back on one another[21,32]: decreased NSC in aboveground woody tissues (e.g., twig, branch, and bole) during extreme droughts was closely tied with reduced xylem resistance to

embolism, impeding the maintenance of turgor and cell metabolism; in turn, reduced hydraulic conductance slowed xylem refilling and regrowth following osmotic regulation and drought relief[32,33]. Our analysis shows that ecosystems displaying hyposensitive canopy stomatal control had lower stability (i.e., the absolute value of R_c–R_t) during droughts than hypersensitive ecosystems (Fig. 3b), suggesting that they might be more susceptible to mortality from extreme, prolonged droughts. This was further supported by the lesser recovery of G_{cref} and NEP to normal the year following droughts (Fig. 3a and Supplementary Fig. 2). Utilizing permissive WUS_e under extreme droughts, thus escaping the consequences of a marked decrease in NEP at the cost of greater risk to the hydraulic system, may be a riskier WUS_e.

These findings suggest that ecosystems can be divided into those which display hyposensitive sensitivity of canopy stomatal conductance to VPD and others showing hypersensitive behavior from the perspective of WUS_e, with the majority of ecosystems behaving in a manner consistent with isohydric regulation of Ψ_x. Ecosystems showing drastically different behavior may facilitate understanding processes responsible for ecosystem dysfunction and allow modeling and predicting ecosystem stability under droughts.

Implications

Long-term additional water supply (e.g., irrigation) in arid and semi-arid regions is widely applied, enhancing ecosystem services by promoting plant growth and yield[34]. Although such management increases plant photosynthetic productivity to some extent, long-term excessive irrigation will result in permissive WUS_e (Fig. 1c), decreasing plant water-use efficiency and further exacerbating regional water deficit. For instance, a large proportion of forest plantations in China's Three-North Shelter Regions are intensively irrigated to ensure survival and enhance multiple ecosystem functions[35]. Such irrigation is conducive to accelerating tree growth by eliminating drought stress in the early stages of stand development. However, the permissive WUS_e developed by additional water supply in these plantations will deplete groundwater, leading to water shortages, while the resulting WUS_e may lead to the death of trees unprepared to withstand extreme droughts[36]. In contrast, unirrigated, water-deficit ecosystems in arid regions are adapted to their growth environment and survive with a relatively conservative WUS_e (Fig. 1c). Furthermore, as suggested by our results, WUS_e in humid regions is generally permissive; a continuous increase in VPD may result in higher water use with consequences to water resources and ecosystem stability in the future.

Declarations

Acknowledgments

This study was supported by the National Natural Science Foundation of China (Grant No. 31872711), the Beijing Municipal Commission of Education (Innovative Transdisciplinary Program of Ecological

Restoration Engineering). In addition, the authors would like to express their appreciation to the US-China Carbon Consortium (USCCC) for constructive suggestions. Special thanks to the data providers of the study sites from the FLUXNET community. We also thank William Anderegg for providing the community-weighted hydraulic trait dataset in our manuscript. Financial support for RO was provided by the Chinese Academy of Sciences President's International Fellowship Initiative, Grant No. 2016VBA036, and the Erkko Visiting Professor Programme of the Jane and Aatos Erkko 375th Anniversary Fund, through the University of Helsinki.

Author contributions

Z.Z., R.O., and H.X. designed the research. H.X. and X.W. collected data and conducted the analysis. Z.Z., R.O., and H.X. interpreted the results and wrote the paper.

Competing interests

The authors declare no competing interests.

Methods

Study sites and data processing. The global ecosystem observation network using the eddy covariance technique (i.e., FLUXNET) provides high-quality and standardized data of carbon and water flux and micrometeorological elements. Here we integrated eddy covariance measurements and micrometeorological observations of 165 ecosystems from the FLUXNET2015 Tier-1 Dataset (http://fluxnet.fluxdata.org/data/fluxnet2015-dataset/) with an open-access policy, remote-sensing products, and plant functional-trait data to explore the drought adaptability of ecosystems with different water-use strategies. Of 165 flux sites, 77 are forest sites consisting of deciduous, broad-leaved forests (DBF; 19), evergreen broadleaved forests (EBF; 12), evergreen needle-leaved forests (ENF; 38), and mixed forests (MF; 8), 13 are savanna sites (SAV), 11 are shrubland sites (SH), 30 are grassland sites (GRA), 18 are cropland sites (CRO), and 16 are wetland sites (WET), representing a total of 1249 site-years of data with widely disparate climate conditions (Supplementary Fig. 1 and Supplementary Table 1). The flux data processing followed a well-established pipeline, including data quality checks, data filtering during low turbulence periods, gap-filling for meteorological and flux measurements, and partitioning of net CO_2 flux into ecosystem respiration (ER) and gross primary productivity (GPP)[37].

Climate region classification and ecosystem water availability. Climate region classification is commonly estimated by aridity index (AI), a numerical indicator measuring the dryness of the climate at a given location, which is quantified by the ratio of the long-term water supply (e.g., precipitation, P) to the long-term climatic water demand (i.e., PET). In this study, we extracted the mean annual aridity index (1970-2000) of each site from the Global Aridity Index and Potential Evapotranspiration (ET_0) Climate Database v2 using QGIS[38]. Then, based on United Nations Environmental Programme[39], we defined the areas with a multi-year average AI of less than 0.65 as arid regions (i.e., drylands) and, otherwise, as humid regions.

The prevailing condition of ecosystem water availability was defined by the Priestley-Taylor coefficient (α) that is the ratio of the actual LE to the equilibrium LE (LE_{eq})[40]. LE_{eq} is the theoretical LE without radiation and temperature limitation over an extensive wet surface and is calculated as follows:

$$LE_{eq} = \frac{\Delta(H+LE)}{\Delta+\gamma} \quad (1)$$

where Δ is the slope of the saturation vapor pressure versus temperature curve (kPa K^{-1}), H and LE indicate the sensible heat (MJ m^{-2} d^{-1}) and the latent heat of vaporization (MJ m^{-2} d^{-1}), respectively. γ is the psychrometric constant (0.066 kPa K^{-1}).

Definition of drought year and drought intensity. We employed the standardized precipitation evapotranspiration index (SPEI) as a measure of drought intensity (i.e., the absolute value of SPEI) across study sites. SPEI is a multiscalar drought index with a resolution of 0.5° from 1982 to 2013 (SPEIbase v.2.5; http://sac.csic.es/spei/database/), taking into account both monthly precipitation and potential evapotranspiration (PET) based on CRU TS3.2 climate data (http://www.cru.uea.ac.uk/cru/data/hrg/) and the FAO-56 Penman-Monteith method, such that the more negative the value is, the more severe the drought is relative to the long-term conditions[41]. We defined a drought year based on SPEI-12, which was extensively adopted to reflect annual water conditions[42]. As the study sites cannot cover the global SPEI grids, we reset the thresholds to distinguish the moderate and extreme drought years according to the probability of the occurrence of drought severity[42]. As a result, the experiment years with SPEI less than −1.5 and −0.75 were identified as extreme and moderate drought years, respectively (Supplementary Fig. 5). Drought intensity was represented by the absolute value of SPEI in this study. Each site with repeated measures (i.e., multiple drought events) is represented by its most severe drought condition. PET for determining the drought index was computed as:

$$PET = \frac{0.408\Delta(H+LE)+\gamma\left(\frac{900}{T_a+273.15}\right)\mu\cdot VPD}{\Delta+\gamma(1+0.34\mu)} \quad (2)$$

where T_a is the air temperature (°C), μ is the wind speed (m s^{-1}), and VPD is the vapor pressure deficit (kPa).

Although an inverse correlation between the prevailing soil moisture and VPD dominates at the regional scale, areas classified as humid or arid, based on long-term precipitation relative to potential evapotranspiration, may both experience a wide range of α. Roughly, the distinction between humid and arid regions emphasizes the long-term atmospheric conditions and, in combination with the index of α, allows a degree of distinction between water stress imposed by the prevailing atmospheric conditions with or without corresponding soil moisture limitation. In addition to these annual-to-interannual metrics, with which one may expect the vegetation to be in some quasi-stable equilibrium, ecosystems may be

subjected to periodic drought, reflecting an imbalance between monthly precipitation and potential evapotranspiration (i.e., SPEI). Such droughts may occur in both types of regions, and regardless of whether the vegetation is in equilibrium with typically high or low soil moisture availability (Supplementary Fig. 6). Although the three metrics are not independent, each carries unique information and allows further assessment of the likely response of vegetation to drought.

Biophysical parameters. The conductance of canopies (G_c, mm s^{-1}) of ecosystems in which the canopies are well-coupled to the atmosphere during the growing season essentially represent the stomata conductance of its leaves[43], which was computed by inverting the Penman-Monteith equation as follows[44]:

$$G_c^{-1} = \frac{\rho_a C_p \left(\frac{VPD}{LE}\right)}{\gamma} + \left(\frac{\Delta}{\gamma}\beta - 1\right) g_a^{-1} \quad (3)$$

$$g_a^{-1} = \frac{\mu}{\mu_*^2} + 6.2\mu_*^{-2/3} \quad (4)$$

where ρ_a is the air density (1.2 kg m^{-3}), C_p is the specific heat capacity of air (1.005 J kg^{-1} K^{-1}), β is the Bowen ratio (i.e., H/LE), g_a is the aerodynamic conductance (mm s^{-1}), and μ* is the friction velocity (m s^{-1}). To compare G_c across sites and assure adequate canopy-atmosphere coupling, G_c was calculated under the reference meteorological conditions (i.e., precipitation = 0 during past ten h, $R_g \geq 400$ W m^{-2}, $u \geq 1$ m s^{-1}) where the canopy was dry and ventilated, and radiation did not limit transpiration[45]. While G_c is not a perfect proxy for g_s because it contains both stomatal and soil conductance to water loss, these interactions can be minimized through careful data screening[46].

For each flux site, we extracted satellite products to characterize the ecosystem LAI. To consider matching the resolution of remote sensing product and flux observation footprint, we used the level-4 MODIS LAI/FPAR product (i.e., MCD15A2) at 1-km spatial resolution and 8-day temporal resolution. In order to exclude the impacts of cloud contamination and atmospheric variability, the noise of the LAI time series was smoothed by the Savitzky-Golay filter in the TIMESAT software (version 3.3)[47]. In this study, we used the anomaly (z-score) of the ratio of LAI to NEP to indicate the proportion of NEP used for aboveground productivity and leaf carbon sequestration efficiency (i.e., leaf area required to fix a unit of carbon).

For each species, P_{50} and HSM were obtained from the Xylem Functional Traits database[48], which are commonly used indices of embolism resistance and hydraulic vulnerability to drought, respectively[7]. Then, we computed the mean values of each trait for each site as the community-weighted mean based on the previous study[49].

Definition of canopy stomatal sensitivity. Stomatal sensitivity is commonly derived from the relative decrease in stomatal conductance with respect to increasing VPD[27]. At each site, we plotted G_c against VPD during the growing seasons (i.e., May-September in the northern hemisphere and September-May of the following year in the southern hemisphere). The half-hourly data under reference meteorological conditions were classified into VPD intervals of 0.2 kPa, starting at 0.6 kPa. We constructed the upper envelopes of the data clouds using the sum of averaged G_c and one standard deviation for all VPD classes. The upper envelope indicated the potential G_c at a given VPD condition, where stomatal behavior is hardly limited by other factors (e.g., light, soil moisture, temperature) at the ecosystem scale[25,45]. An empirical function was fitted to the envelopes[25]:

$$G_c = -m \cdot \ln(VPD) + G_{cref} \quad (5)$$

where m is the $dG_c/d\ln(VPD)$ (mm s^{-1} $\ln(kPa)^{-1}$), and G_{cref} is the reference canopy conductance (G_c at VPD = 1 kPa, mm s^{-1}).

When stomata can maintain the difference between soil and leaf water potential despite changes in VPD, canopy conductance and atmospheric evaporative demand are coupled to water potential along the soil-plant-atmosphere continuum by the following relationship[50]:

$$g_{su} = \left(\frac{\lambda\gamma}{C_p\rho}\right)\left(\frac{K}{A}\right)\frac{1}{VPD}(\psi_s - \psi_l) \quad (6)$$

where g_{su} is the surface conductance (i.e., the total ecosystem-atmosphere conductance, mm s^{-1}), indicating g_a and G_c in series ($g_{su}=(g_a^{-1}+G_c^{-1})^{-1}$), Ψ_s and Ψ_l are soil and leaf water potential, respectively, K/A is the hydraulic conductance of the soil-to-canopy pathway (i.e., water flux per time, per leaf area, and per water potential gradient, mm s^{-1}). At the canopy scale, K/A can be written as the ratio of water flux (i.e., evapotranspiration, ET) per ground surface area to water potential gradient during the growing season when plant transpiration dominates ecosystem water loss[43,50]. Thus, we calculated the theoretical G_c at each VPD value and estimated the theoretical ratio for each site based on Eq. 6.

In this study, we used the normalized residual (i.e., the residual from the 1:1 line / the expected value on the line) to represent canopy stomatal sensitivity (S_c) reflecting ecosystem water-use strategy (WUS_e) following a framework for distinguishing plant hydraulic behaviors[25]. Given the uncertainty in calculations, we regarded the ecosystems falling within 5% of the 1:1 line as isohydric ecosystems. Where S_c was less than −0.05 for a specific ecosystem (i.e., below the lower dashed line), it was considered having weak canopy stomatal control and defined a hyposensitive ecosystem; where S_c was greater than 0.05 (i.e., above the upper dashed line), it was considered very sensitive to VPD, defined a hypersensitive ecosystem (Fig. 4).

Ecosystem stability. Ecosystem stability during extreme climate events relies on both R_t and R_c. R_t and R_c indicate the ability of an ecosystem to persist through an extreme climatic event and to recover from an event to its normal state, respectively[42]. We defined R_t and R_c in this study as follows[42]:

$$R_t = \frac{\overline{P_n}}{|P_d - \overline{P_n}|} \quad (7)$$

$$R_c = \frac{|P_d - \overline{P_n}|}{|P_{d+1} - \overline{P_n}|} \quad (8)$$

where $\overline{P_n}$, P_d, and P_{d+1} are the mean multi-year expected NEP during normal years (i.e., non-drought event years), during a drought year, and the year after drought, respectively. The R_t and R_c are dimensionless, which are comparable across sites with different NEP levels directly. Also, they are robust for analyzing dynamic systems displaying either a monotonous recovery or damped oscillations following a climatic disturbance[42].

Statistical analysis. Analysis of covariance (ANCOVA) was conducted to evaluate the significance of differences in NEP and G_{cref} anomaly responses to drought severity between hyposensitive and hypersensitive ecosystems. Independent-sample and one-sample t-*test* analysis was used to assess the significance of differences in the means of two sets of variables and the mean of sample data to a specific value, respectively. In addition, Pearson correlation analysis was performed to evaluate the correlation coefficient (r) between two variables. All statistical analyses above were performed using SPSS (version 22.0, Chicago, IL, USA). Regression models were calculated by using R 3.6.2.

References

1. Bennett, A. C., Mcdowell, N. G., Allen, C. D. & Anderson-Teixeira, K. J. Larger trees suffer most during drought in forests worldwide. *Nat. Plants* **1**, 1–5 (2015).
2. Anderegg, W. R. L. *et al*. Meta-analysis reveals that hydraulic traits explain cross-species patterns of drought-induced tree mortality across the globe. *Proc. Natl. Acad. Sci. U. S. A.* **113**, 5024–5029 (2016).
3. Anderegg, W. R. L. *et al*. Tree mortality predicted from drought-induced vascular damage. *Nat. Geosci.* **8**, 367–371 (2015).
4. Anderegg, W. R. L., Kane, J. M. & Anderegg, L. D. L. Consequences of widespread tree mortality triggered by drought and temperature stress. *Nat Clim Change* **3**, 30–36 (2013).
5. Feng, X. *et al*. The ecohydrological context of drought and classification of plant responses. *Ecol. Lett.* **21**, 1723–1736 (2018).
6. Allen, C. D. *et al*. A global overview of drought and heat-induced tree mortality reveals emerging climate change risks for forests. *For. Ecol. Manage* **259**, 660–684 (2010).

7. Choat, B. *et al*. Global convergence in the vulnerability of forests to drought. *Nature* **491**, 752–755 (2012).
8. McDowell, N. G. et al. Evaluating theories of drought-induced vegetation mortality using a multimodel-experiment framework. *New Phytol.* **200**, 304–321 (2013).
9. Powell, T. L. et al. Confronting model predictions of carbon fluxes with measurements of Amazon forests subjected to experimental drought. *New Phytol.* **200**, 350–365 (2013).
10. Trugman, A. T., Anderegg, L. D. L., Anderegg, W. R. L., Das, A. J. & Stephenson, N. L. Why is Tree Drought Mortality so Hard to Predict? *Trends Ecol. Evol.* **36**, 520–532 (2021).
11. Gupta, A., Rico-Medina, A. & Caño-Delgado, A. I. The physiology of plant responses to drought. *Science* **368**, 266–269 (2020).
12. Zhou, S., Zhang, Y., Williams, A. P. & Gentine, P. Projected increases in intensity, frequency, and terrestrial carbon costs of compound drought and aridity events. *Sci. Adv.* **5**, 1–9 (2019).
13. Reichstein, M. *et al*. Climate extremes and the carbon cycle. *Nature* **500**, 287–295 (2013).
14. Grossiord, C. *et al*. Plant responses to rising vapor pressure deficit. *New Phytol.* **226**, 1550–1566 (2020).
15. Yuan, W. *et al*. Increased atmospheric vapor pressure deficit reduces global vegetation growth. *Sci. Adv.* **5**, eaax1396 (2019).
16. Oishi, A. C., Oren, R., Novick, K. A., Palmroth, S. & Katul, G. G. Interannual invariability of forest evapotranspiration and its consequence to water flow downstream. *Ecosystems* **13**, 421–436 (2010).
17. Choat, B. *et al*. Triggers of tree mortality under drought. *Nature* **558**, 531–539 (2018).
18. Flo, V. *et al*. Climate and functional traits jointly mediate tree water use strategies. *New Phytol.* **231**, 617–630 (2020).
19. Feng, X. *et al*. Beyond isohydricity: The role of environmental variability in determining plant drought responses. *Plant Cell Environ.* **42**, 1104–1111 (2019).
20. Hochberg, U., Rockwell, F. E., Holbrook, N. M. & Cochard, H. Iso/Anisohydry: A Plant-Environment Interaction Rather Than a Simple Hydraulic Trait. *Trends Plant Sci.* **23**, 112–120 (2018).
21. Garcia-Forner, N., Biel, C., Savé, R. & Martínez-Vilalta, J. Isohydric species are not necessarily more carbon limited than anisohydric species during drought. *Tree Physiol.* **37**, 441–455 (2017).
22. Feng, X. *et al*. Beyond isohydricity: The role of environmental variability in determining plant drought responses. *Plant Cell Environ*. **42**, 1104–1111 (2019).
23. McDowell, N. *et al*. Mechanisms of plant survival and mortality during drought: Why do some plants survive while others succumb to drought? *New Phytol.* **178**, 719–739 (2008).
24. Martínez-Vilalta, J. & Garcia-Forner, N. Water potential regulation, stomatal behaviour and hydraulic transport under drought: deconstructing the iso/anisohydric concept. *Plant Cell Environ.* **40**, 962–976 (2017).

25. Oren, R. *et al*. Survey and synthesis of intra- and interspecific variation in stomatal sensitivity to vapour pressure deficit. *Plant, Cell Environ.* **22**, 1515–1526 (1999).
26. Borghetti, M., Gentilesca, T., Leonardi, S., Van Noije, T. & Rita, A. Long-term temporal relationships between environmental conditions and xylem functional traits: A meta-analysis across a range of woody species along climatic and nitrogen deposition gradients. *Tree Physiol.* **37**, 4–17 (2017).
27. Novick, K. A. *et al*. The increasing importance of atmospheric demand for ecosystem water and carbon fluxes. *Nat. Clim. Change* **6**, 1023–1027 (2016).
28. Chen Y. J. *et al.* Hydraulic prediction of drought-induced plant dieback and top-kill depends on leaf habit and growth form. *Ecol. Lett*. (2021).
29. Hartmann, H. & Trumbore, S. Understanding the roles of nonstructural carbohydrates in forest trees-from what we can measure to what we want to know. *New Phytol.* **211**, 386–403 (2016).
30. Klein, T., Hoch, G., Yakir, D. & Körner, C. Drought stress, growth and nonstructural carbohydrate dynamics of pine trees in a semi-arid forest. *Tree Physiol.* **34**, 981–992 (2014).
31. Rowland, L. *et al*. Death from drought in tropical forests is triggered by hydraulics not carbon starvation. *Nature* **528**, 119–122 (2015).
32. Sevanto, S., Mcdowell, N. G., Dickman, L. T., Pangle, R. & Pockman, W. T. How do trees die? A test of the hydraulic failure and carbon starvation hypotheses. *Plant, Cell Environ.* **37**, 153–161 (2014).
33. Adams, H. D. *et al*. A multi-species synthesis of physiological mechanisms in drought-induced tree mortality. *Nat. Ecol. Evol.* **1**, 1285–1291 (2017).
34. Walker, B. H. Management of semi-arid ecosystems. (Elsevier, Amsterdam, 2012).
35. State Forestry Administration. Reports of forestry resources in China. Chinese Forestry Press (2013).
36. Cao, S. *et al*. Excessive reliance on afforestation in China's arid and semi-arid regions: Lessons in ecological restoration. *Earth-Science Reviews***104**, 240-245 (2011).
37. Pastorello, G. *et al*. The FLUXNET2015 dataset and the ONEFlux processing pipeline for eddy covariance data. *Sci. Data* **7**, 225 (2020).
38. Trabucco, A. & Zomer, R. Global Aridity Index and Potential Evapotranspiration (ET0) Climate Database v2. *CGIAR Consort. Spat. Inf.* **10** (2019).
39. UNEP. World atlas of desertification 2ed. United Nations Environ. Program. (1997).
40. Priestley, C. H. B. H. B., Physics, R. J. T. A., Taylor, R. J., Priestley, C. H. B. H. B. & Taylor, R. J. On the assessment of surface heat flux and evaporation using large-scale parameters. *Mon. Weather Rev.* **100**, 81–92 (1972).
41. Beguería, S., Vicente-Serrano, S. M., Reig, F. & Latorre, B. Standardized precipitation evapotranspiration index (SPEI) revisited: Parameter fitting, evapotranspiration models, tools, datasets and drought monitoring. *Int. J. Climatol.* **34**, 3001–3023 (2014).
42. Isbell, F. *et al*. Biodiversity increases the resistance of ecosystem productivity to climate extremes. *Nature* **526**, 574–577 (2015).

43. Xu, H. *et al*. Environmental and canopy stomatal control on ecosystem water use efficiency in a riparian poplar plantation. *Agric. For. Meteorol.* **287**, 107953 (2020).
44. Monteith, J. & Unsworth, M. Principles of Environmental Physics: Plants, Animals, and the Atmosphere: 4th ed. (Academic Press, London, 2013).
45. Xu, H. *et al*. Canopy photosynthetic capacity drives contrasting age dynamics of resource use efficiencies between mature temperate evergreen and deciduous forests. *Glob. Chang. Biol.* **26**, 6156–6167 (2020).
46. Kim, D. *et al*. Sensitivity of stand transpiration to wind velocity in a mixed broadleaved deciduous forest. *Agric. For. Meteorol.* **187**, 62–71 (2014).
47. Jönsson, P. & Eklundh, L. TIMESAT - A program for analyzing time-series of satellite sensor data. *Comput. Geosci.* **30**, 833–845 (2004).
48. Gleason, S. M. *et al*. Weak tradeoff between xylem safety and xylem-specific hydraulic efficiency across the world's woody plant species. *New Phytol.* **209**, 123–136 (2016).
49. Anderegg, W. R. L. *et al*. Hydraulic diversity of forests regulates ecosystem resilience during drought. *Nature* **561**, 538–541 (2018).
50. Herbst, M., Rosier, P. T. W., Morecroft, M. D. & Gowlng, D. J. Comparative measurements of transpiration and canopy conductance in two mixed deciduous woodlands differing in structure and species composition. *Tree Physiol.* **28**, 959–970 (2008).

Figures

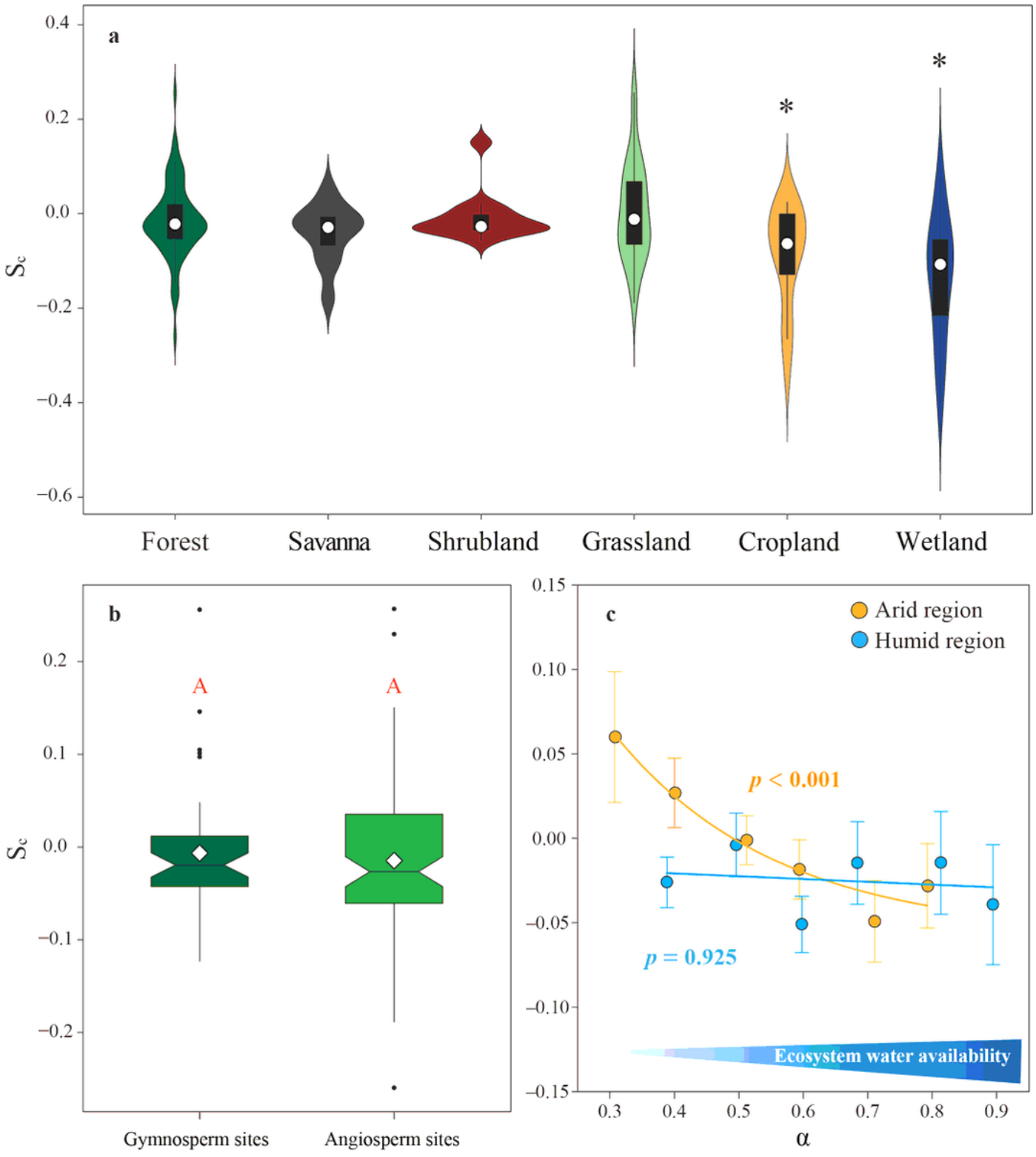

Figure 1

Variation of Sc with ecosystem types (a), hydraulic traits (b), and water availability (c). (a) Violin diagrams show the distribution of Sc for different ecosystems. The hollow circle represents the median. The asterisk above the violins indicates the ecosystem type in which there was a significant difference at the significance level of 0.05 between the empirical m/Gcref and the theoretical ratio. (b) Boxplots showing Sc for angiosperm-dominated (green) and gymnosperm-dominated (dark green) ecosystems.

Notches approximate the 95% confidence interval for the median, and whiskers extend to the highest and lowest values within 1.5 times the interquartile range (IQR) of the upper and lower quartiles. The diamond in each box is the mean value. (c) Relationship between Sc and α in humid regions (Sc = −0.017α − 0.014; R2 = 0.03) and arid regions (Sc = −0.06 + 0.40e−3.99α; R2 = 0.95), respectively. Sc values were binned into 0.1 α increments. Error bar is the standard error of the mean in each bin.

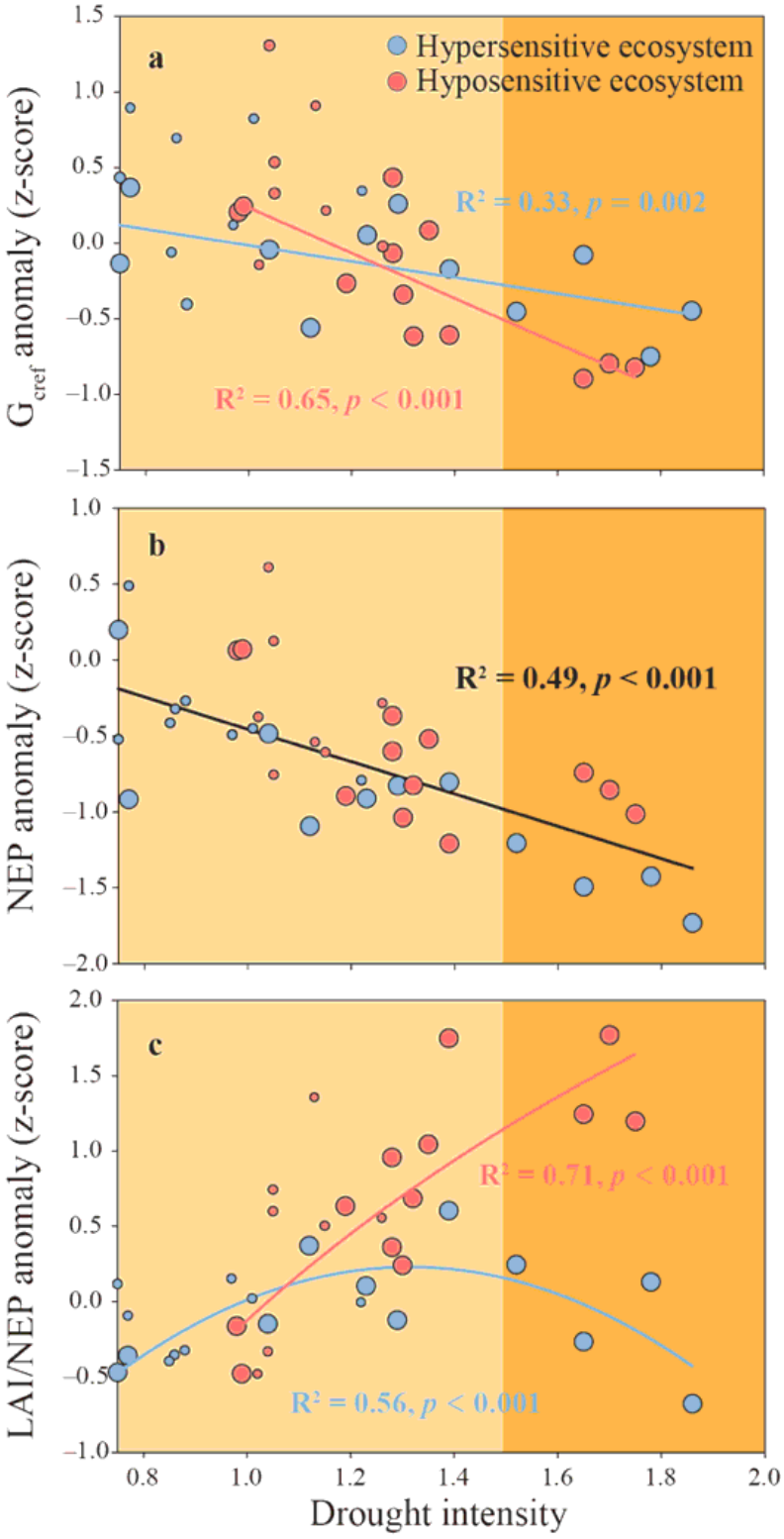

Figure 2

Relationships between anomalies (z-score) of annual (a) Gcref, (b) NEP, and (c) LAI/NEP and drought intensity (i.e., the absolute value of SPEI) for hypersensitive (blue) and hyposensitive ecosystems (red). Light and dark orange areas indicated moderate and extreme drought conditions, respectively. Smaller circles of the same color represent repeated measures (i.e., drought events) for some sites but are not included in the regression analyses.

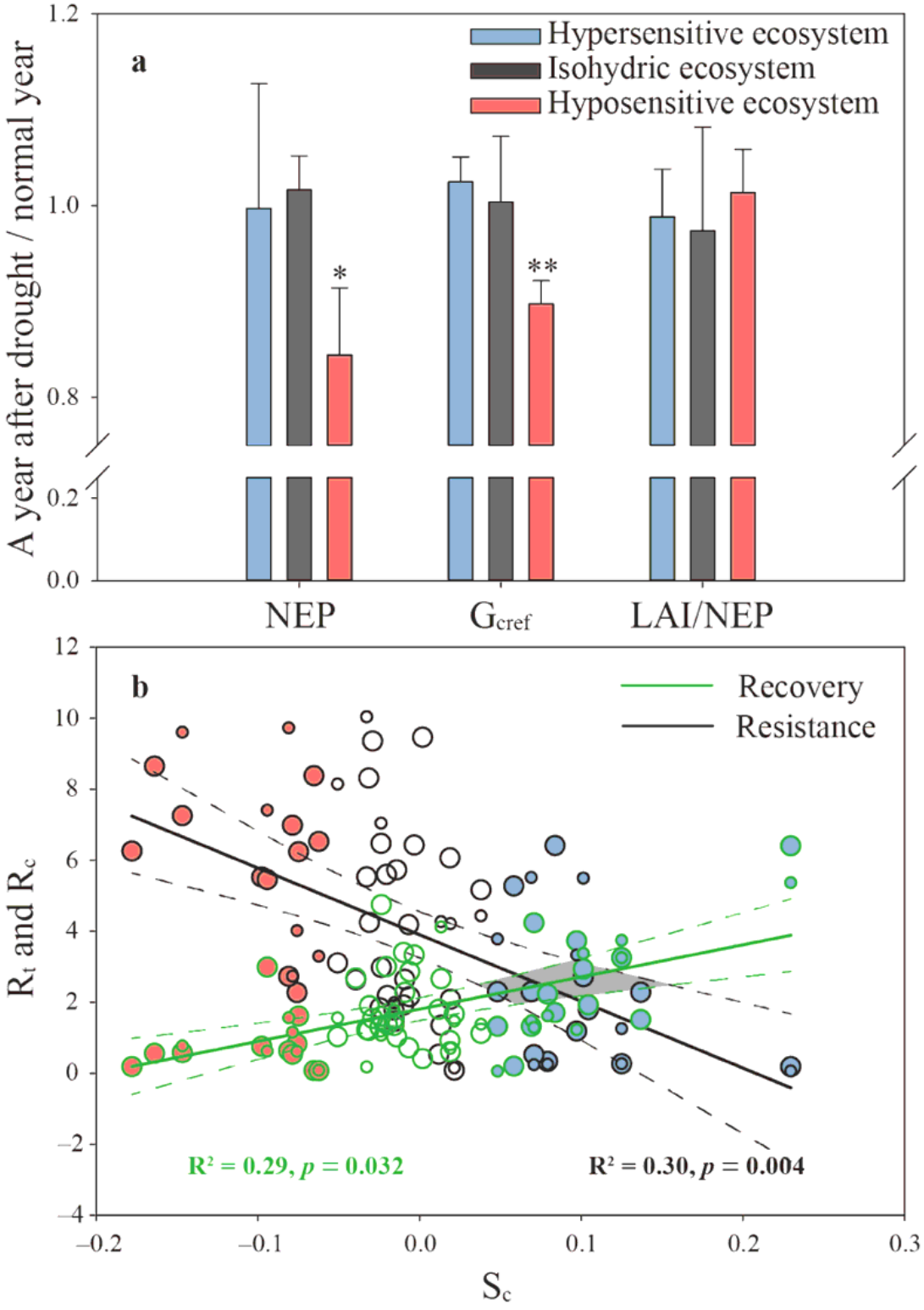

Figure 3

Ecosystem stability in response to drought. (a) Ratios of NEP, Gcref, and the ratio of LAI to NEP of the year following a drought year to the multi-year mean of non-drought years for hypersensitive (blue) and hyposensitive ecosystems (red) across the sites experiencing droughts, with isohydric ecosystems for reference (gray). "*" and "**" above bars indicate the significance of the difference from unity at the level of 0.05 and 0.01, respectively. (b) The sensitivity of ecosystem recovery Rc (green line) and resistance Rt (black line) to Sc across following droughts at all flux observation sites. Red, white, and blue circles represent hyposensitive, isohydric, and hypersensitive ecosystems, respectively. The range between the two dashed lines indicates the 95% confidence interval. Smaller circles of the same color represent repeated measures (i.e., drought events) for some sites but are not included in the regression analyses.

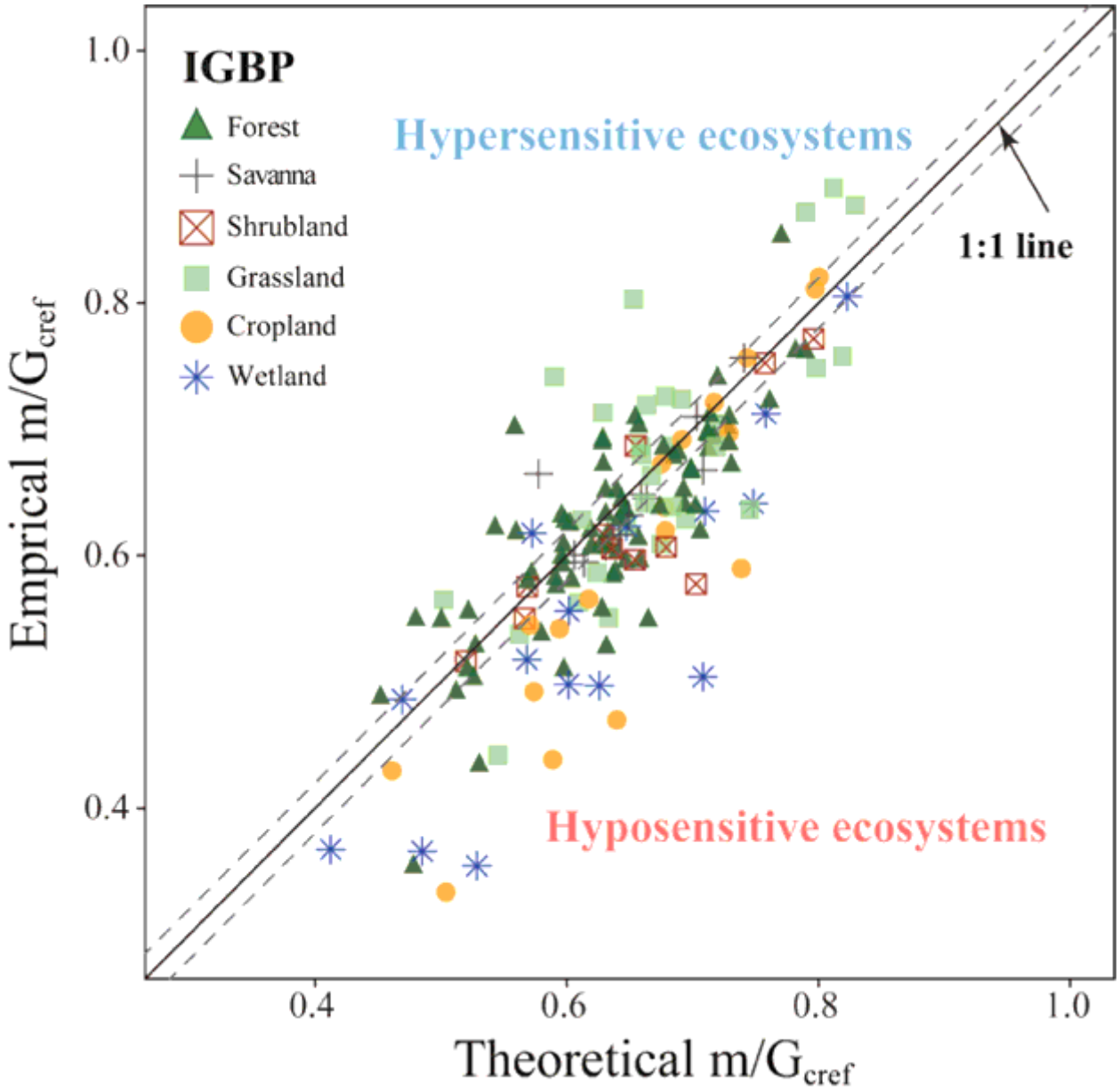

Figure 4

Relationship between the empirical ratio of dGc/dln(VPD) (m) to reference canopy conductance (Gcref) and the theoretical value across 165 ecosystems.

Supplementary Files

This is a list of supplementary files associated with this preprint. Click to download.

- SupplementaryMaterial.docx